DIRECT NONLINEAR POWER MESFET PARAMETER EXTRACTION AND CONSISTENT MODELING

A. Werthof, F. van Raay, and G. Kompa

University of Kassel, Department of High-Frequency Engineering
Wilhelmshöher Allee 73, DW-3500 Kassel, Germany

ABSTRACT

A new method is developed which permits a direct nonlinear FET parameter extraction of the gate source capacitor and diode, the drain current generator and the avalanche breakdown characteristics from large-signal waveform measurements. Differences between the DC and RF characteristics of the drain current generator and the breakdown characteristics are observed and interpreted. The measured FET output power and phase spectra are compared with the simulated results for different RF models of the nonlinear drain current generator. The proposed method is a valuable instrument for the analysis of the actually existing high frequency FET nonlinearities and can be helpful in the improvement of large-signal FET models.

INTRODUCTION

The simulation and design of nonlinear microwave circuits require reliable large-signal FET models. The parameters for the nonlinear FET models which are implemented in commercially available nonlinear circuit simulators are usually extracted from the measured DC or pulsed DC characteristics and from the S-parameters [1]. The approximation of the nonlinear characteristics with analytical functions and the neglection of the differences between the DC and RF characteristics of the drain current generator can lead to inaccurate simulation results [2].

In [3] a method has been proposed which additionally takes into account the RF output power spectra measured under large-signal operating conditions. The coefficients of analytical functions used to model the FET nonlinearities are fitted to match not only the measured DC characteristics and S-parameters but also the RF output power spectra. This approach is based on the assumption that the analytical functions are appropriate to describe the S-parameters, the DC and the nonlinear RF characteristics simultaneously which often may suffer from the FET low frequency dispersion phenomena.

To overcome these limitations, we follow a new extraction concept which allows a direct nonlinear FET parameter extraction without the necessity of the above mentioned assumptions. Precisely measured voltage and current spectra transformed from the outer to the inner FET reference planes are used for the analysis of the measured nonlinear RF characteristics of the voltage controlled drain current generator.

T

NONLINEAR DEEMBEDDING PROCEDURE

The fundamental data of the proposed extraction method are the DC characteristics, the S-parameters of different DC bias points and the voltage and current spectra in the outer FET gate and drain reference planes (Figure 1) for different DC bias points, RF input power levels and fundamental frequencies. The FET voltage and current spectra

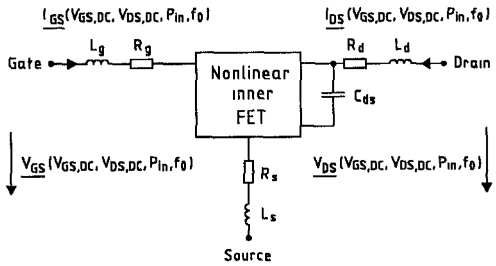

Figure 1: Outer FET reference planes.

$(\underline{V_{GS}}, \underline{I_{GS}}, \underline{V_{DS}}, \underline{I_{DS}})$ were measured in a large-signal waveform measurement system [4] with 40 GHz harmonic bandwidth. The FET small signal equivalent circuit elements were obtained by a highly consistent extraction method described earlier in [5]. The bias dependent small signal equivalent circuit elements (g_m, G_{ds}, C_{gs}, C_{gd}, τ, R_i) were extracted from the S-parameters of multiple different DC bias points, interpolated with 2-d splines and transformed to the inner FET voltage planes V_{gs} and V_{ds} shown in figure 2.

The transformation of the measured voltage and current spectra from the outer to the inner FET reference planes starts with a deembedding of the linear equivalent circuit elements (R_g, R_d, R_s, L_g, L_d, L_s, C_{ds}). The measured spectra are transformed for each DC bias point, RF input power level and frequency component through the linear elements. After the transformation, the measured spectra $(\underline{V'_{GS}}, \underline{I'_{GS}}, \underline{V_{ds}}, \underline{I'_{DS}})$ of the nonlinear inner part of the FET equivalent circuit model (Figure 2) are available. The gate source diode is approximated with the PN diode model. The corresponding

CH3277-1/93/0000-0645$01.00 © 1993 IEEE

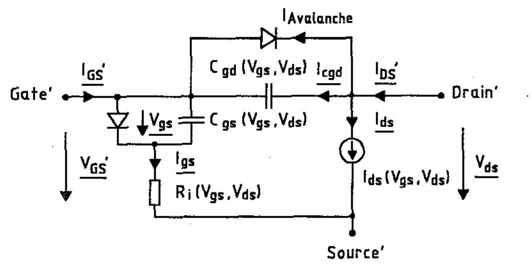

Figure 2: Nonlinear inner part of the FET large-signal equivalent circuit model.

parameters are extracted from the complex signal spectra measured under gate forward operating conditions in a harmonic balance process taking into account bias dependent equivalent circuit elements C_{gs}, R_i, and C_{gd}.

With the parameters of the gate source diode and the bias dependent incremental values of C_{gs} and R_i known, the control voltage V_{gs} over the gate source capacitor C_{gs} can be derived from the measured gate voltage spectra $\underline{V'_{GS}}$ with a harmonic balance solution of the equation

$$V'_{GS} = V_{gs} + R_i(V_{gs}, V_{ds})\, I_{gs}\,. \qquad (1)$$

The current $I_{gs,C_{gs}}$ through the gate source capacitor C_{gs} can be calculated from the measured gate current spectra $\underline{I'_{GS}}$ with a deembedding of the gate drain capacitor C_{gd} and the gate source diode,

$$I_{gs,C_{gs}} = I'_{GS} + C_{gd}(V_{gs}, V_{ds})\frac{d(V_{ds} - V'_{GS})}{dt} - I_{gs,diode}\,. \qquad (2)$$

The current of the gate drain capacitor is calculated as the product of the bias dependent incremental C_{gd} values with the derivative of the measured differences between the gate and drain voltages with respect to the time. The characteristic of the gate source capacitor is calculated from the deembedded measured gate voltage and current spectra using the equation

$$C_{gs}(V_{gs}, V_{ds}) = I_{gs,C_{gs}}/(dV_{gs}/dt)\,. \qquad (3)$$

The measured drain current spectra $\underline{I'_{DS}}$ are corrected for the current through the feedback capacitor C_{gd},

$$I_{ds} = I'_{DS} - C_{gd}(V_{gs}, V_{ds})\frac{d(V_{ds} - V'_{GS})}{dt}\,. \qquad (4)$$

The effect of the control voltage V_{gs} on the drain current generator is taken into account by a nonlinear time delay $\tau(V_{gs}, V_{ds})$. The control voltage

$$V_{gs}(t_i - \tau(V_{gs(t_i)}, V_{ds(t_i)}) = \mathcal{F}^{-1}(\underline{V_{gs}}\, e^{-j\omega\tau(V_{gs}(t_i), V_{ds}(t_i))}) \qquad (5)$$

can be calculated in the time domain for each time sample t_i.

The construction of the nonlinear RF drain current generator characteristics has been accomplished by analyzing the deembedded signal waveforms for different input power levels and DC bias points. To permit a direct comparison with the measured DC characteristics, the evaluation has been carried out for defined values of the instantaneous gate control voltage V_{gs}. The corresponding values of the output voltage V_{ds} and the drain current I_{ds} are determined from the deembedded waveforms at those specific time points at which the gate control voltage has reached the above mentioned defined values. The extracted characteristics have been found as being really significant under large-signal operating conditions. They can be directly implemented in a large-signal FET model or utilized to analyze the validity not only of analytical but of arbitrary functions which are used to calculate the RF drain current characteristic as a function of the measured inner voltage spectra $\underline{V_{gs}}$ and $\underline{V_{ds}}$.

POWER MESFET EXAMPLE

The voltage and current spectra of a power GaAs MESFET of type Toshiba JS8836 were measured at a fundamental frequency of 3 GHz and the operating conditions $V_{GS,DC}$=-2.5V, $V_{DS,DC}$=8V and different RF input power levels (P_{in}=10dBm, ...(1)..., 23dBm). Figure 3 shows the measured DC and the extracted RF characteristics of the nonlinear drain current generator for the defined inner gate voltages. The negative channel conductance of the DC char-

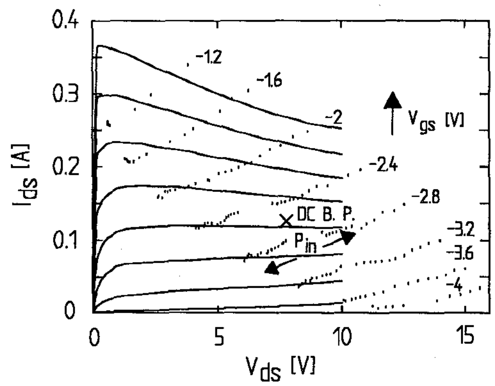

Figure 3: Measured DC (–) and RF (···) characteristics of the nonlinear power MESFET drain current generator.

acteristic for higher gate voltages does not appear in the RF characteristic, because the FET channel temperature is approximately constant during the CW-RF excitation. The RF behaviour agrees with the DC characteristic only for instantaneous voltages near the gate and drain bias values and low input power levels. An increasing deviation can be observed with growing difference between instantaneous and bias voltages which originates in temperature and low frequency dispersion phenomena [2]. The $I_{ds} - V_{ds}$ cross marked traces in Figure 4 represent the results obtained under similar conditions due to Figure 3 with the exception that the DC drain voltage $V_{DS,DC}$ was changed to 6V. The observed dependence of the RF characteristics on the DC drain bias voltage originates in the relatively high and bias dependent

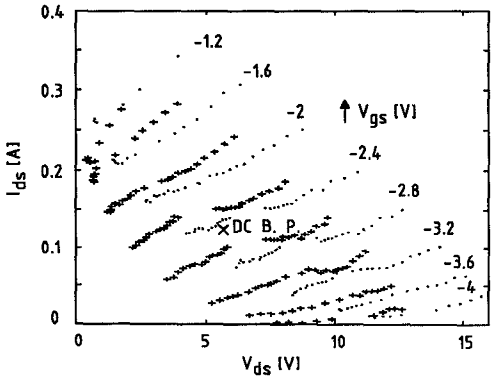

Figure 4: Extracted RF characteristics of the nonlinear power MESFET drain current generator for the DC drain bias voltage $V_{DS,DC}$=6V (+) (dotted traces from Figure 3 for comparison).

power MESFET channel conductance $G_{ds,RF}$. This effect is less visible in typical small-signal FETs [6] because of their lower channel conductance. It may be concluded from our experimental work that analytical functions can only be used to model the RF characteristics of the drain current generator for one given DC bias point.

Figure 5 shows the gate drain avalanche breakdown characteristic, which is one limiting factor in power MESFETs. As can be seen from the extracted results, the RF measurements allow much higher instantaneous avalanche current values without destroying the FET. In contrast to the strong dependence of the DC avalanche breakdown current on the gate bias voltage, the results shown here indicate that the RF avalanche current is mainly dependent only on the gate drain voltage.

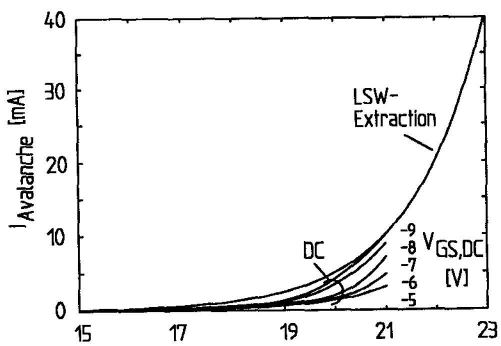

Figure 5: Measured DC and large-signal waveform (LSW) avalanche breakdown currents.

MODELING OF THE NONLINEAR DRAIN CURRENT GENERATOR

Figure 3 illustrates that there are significant differences between the DC and RF characteristics of the nonlinear drain current generator. The question arises, which model can be used to simulate the large-signal RF behaviour. The first model [7] we investigated is based on a consistent formulation for the nonlinear drain current generator. The drain current

$$\begin{aligned} I_{ds,RF}(V_{gs}(t-\tau),V_{ds}) &= I_{ds,DC}(V_{gs}(t-\tau),V_{ds}) \\ &+ I_{kor}(V_{gs}(t-\tau),V_{ds}) \\ &- \frac{1}{T}\int_0^T I_{kor}(V_{gs}(t-\tau),V_{ds})\,dt, \end{aligned} \tag{6}$$

$$\begin{aligned} I_{kor}(V_{gs}(t-\tau),V_{ds}) =& \\ &\int_{V_{gs,DC}}^{V_{gs}(t-\tau)} (g_{m,RF}(v,V_{ds,DC}) - g_{m,DC}(v,V_{ds,DC}))\,dv \\ +& \int_{V_{ds,DC}}^{V_{ds}} (G_{ds,RF}(V_{gs},v) - G_{ds,DC}(V_{gs},v))\,dv \end{aligned}$$

is a combination of the measured DC characteristics and a RF input power dependent correction current term comprising an integral of the differences between the DC and RF transconductance and conductance of the drain current generator from the bias point to the instantaneous voltages. The second model was originally proposed by [8] and is basically also applied in [9,10]. The instantaneous RF drain current of the second model

$$\begin{aligned} I_{ds,RF}(V_{gs},V_{ds}) &= \int_{V_{gs,DC}}^{V_{gs}} g_{m,RF}(v,V_{ds,DC})\,dv \\ &+ \int_{V_{ds,DC}}^{V_{ds}} G_{ds,RF}(V_{gs},v)\,dv \\ &+ I_{ds}(V_{gs,DC},V_{ds,DC}) \end{aligned} \tag{7}$$

is calculated as the integral of the high frequency bias dependent incremental transconductance and output conductance of the drain current generator from the DC bias point to the instantaneous voltages. A simple thermal model was used to correct the values of $g_{m,RF}$ and $G_{ds,RF}$ to account for the fact that the state of thermal equilibrium in the device was different for each bias point with respect to the large-signal operating conditions. The adjustments were performed relative to the DC bias point of the large-signal simulation by assuming the incremental values of the transconductance and conductance to be inversely proportional to the absolute temperature. Figure 6 shows the measured and simulated output power of the first harmonic and figures 7 and 8 the output power and phase of the third harmonic.

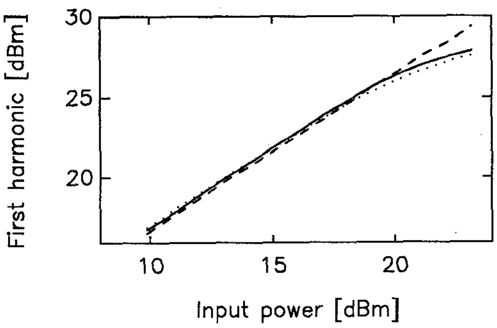

Figure 6: Measured (–) and simulated (eq. 6 (· · ·), eq. 7 (- -)) output power of the first harmonic.

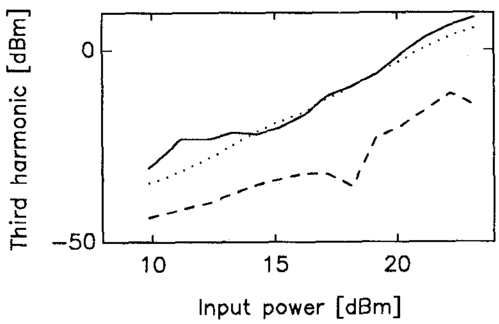

Figure 7: Measured (–) and simulated (eq. 6 (· · ·), eq. 7 (- -)) output power of the third harmonic.

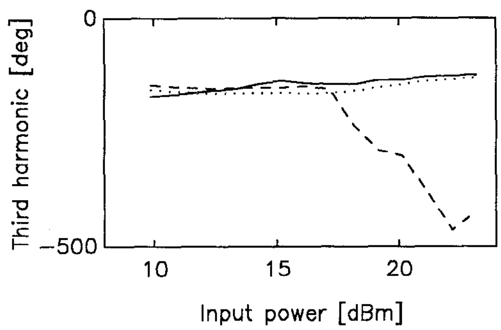

Figure 8: Measured (–) and simulated (eq. 6 (· · ·), eq. 7 (- -)) phase of the third harmonic.

The agreement between measurement and simulation is excellent for the first model. The second model shows a larger disagreement, because the measured DC drain current was used for the integration constant ($I_{ds}(V_{gs,DC}, V_{ds,DC})$) in equation 7. An alternative approach is to set the integration constant equal to the integral of the RF transconductance and channel conductance from pinch-off to the DC bias point. This results in a ficticious DC drain current which is different from the measured DC current due to low frequency dispersion phenomena. The integral of the bias dependent power MESFET RF transconductance from pinch-off to the DC bias point is larger than the measured DC current, which is in contrast to typical small-signal FETs. Because of this characteristic the simulation yields partially negative instantaneous RF drain currents for high input power levels which reduce the input power dependent mean value of the drain current. The reduced mean value results in a too low decrease of the gate control voltage $V_{gs,DC}$ with increasing input power through the feedback effect of the source resistance R_s and is the reason why the simulation shows not the correct compression characteristic. This example demonstrates the importance of the integration constant in equation 7 for a practical nonlinear simulation, a problem which does not occure in the consistent formulation of equation 6.

CONCLUSION

We presented a new method for the direct parameter extraction of the essential power MESFET nonlinearities from large-signal waveform measurements. The measured RF characteristics of the nonlinear drain current generator illustrated the differences between the DC and RF characteristics. The simulated results of two different RF models for the nonlinear drain current generator were compared with the measured complex signal spectra and the importance of the integration constant in equation 7 was emphasized.

REFERENCES

[1] W. R. Curtice, "Active device modeling for GaAs MMIC's," *1992 IEEE MTT-S Symp., Workshop on MMIC design techniques for first-pass success,* Albuquerque, New Mexico, 1992.

[2] J. M. Golio, M. G. Miller, G. N. Maracas, and D. A. Johnson, "Frequency-dependent electrical characteristics of GaAs MESFETs," *IEEE Trans. on Electron Devices,* pp. 1217-1226, 1990.

[3] J. W. Bandler, Q. Zhang, S. Ye, and S. H. Chen, "Efficient large-signal FET parameter extraction using harmonics," *IEEE Trans. Microwave Theory Tech.,* pp. 2099-2108, 1989.

[4] F. van Raay and G. Kompa, "A new on-wafer large-signal waveform measurement system with 40 GHz harmonic bandwidth," *1992 IEEE MTT-S Symp. Dig.,* pp. 1435-1438, 1992.

[5] G. Kompa and M. Novotny, "Highly consistent FET model parameter extraction based on broadband S-parameter measurements," *1992 IEEE MTT-S Symp. Dig.,* pp. 293-296, 1992.

[6] A. Werthof, F. van Raay, and G. Kompa, "Direct nonlinear FET parameter extraction using large-signal waveform measurements," *IEEE Microw. & Guided Wave Letters,* to be published.

[7] A. Werthof and G. Kompa, "A unified consistent DC to RF large signal FET model covering the strong dispersion effects of HEMT devices," *22nd European Microwave Conf. Proc.,* Helsinki, Finland, pp. 1091-1096, 1992.

[8] C. Rauscher and H. A. Willing, "Simulation of nonlinear microwave FET performance using a quasi-static model," *IEEE Trans. Microwave Theory Tech.,* pp. 834-840, 1979.

[9] D. E. Root, S. Fan, and J. Meyer, "Technology independent large signal non quasi-static FET models by direct construction from automatically characterized device data," *21st European Microwave Conf. Proc.,* Stuttgart, Germany, pp. 927-932, 1991.

[10] I. Corbella, J. M. Legido, and G. Naval, "Instantaneous model of a MESFET for use in linear and nonlinear circuit simulations," *IEEE Trans. Microwave Theory Techn.,* pp. 1410-1421, 1992.